Design and Implementation of Ultra-Compact Grating-Based 2x2 Beam Splitter for Miniature Photonic Integrated Circuits

Chin-Hui Chen, Jonathan Klamkin, Leif A. Johansson, and Larry. A. Coldren
Department of Electrical and Computer Engineering, University of California, Santa Barbara, CA 93106
Phone: 805.893.5955, Fax: 805.893.4500, Email: janet@ece.ucsb.edu

Abstract: We provide detailed experimental study of reflectivity, insertion loss, and interference extinction ratio for our recently proposed and demonstrated grating-based beam splitter. Both low-loss and high-extinction-ratio devices are demonstrated for reflectivities close to 50%.

OCIS codes: (130.3120) Integrated optics devices; (230.1360) Beam splitters

1. INTRODUCTION

As the Photonic Integrated Circuits (PICs) become more complex, a demand for smaller and more efficient optical devices increases. This is particularly true for integrated-optic beam splitters, which play an important role in reducing the size of our Coherent Optical Integrated Receiver (CHOIR) PIC [1], [2]. Here, a very compact size of the beam splitter is essential not only for reducing the physical dimension of the PIC, but also for enabling the stability of the PIC at higher frequencies via decreasing the delay in the optical feedback circuit [1]. The recently proposed grating-based beam splitter [2] has been demonstrated to have a superior ultra-short splitting length of only 10 μm. Although the grating-based beam splitter is considerably smaller than its conventional counterparts, it requires a comparable fabrication complexity. Also, it can achieve high throughput, while many other advanced technologies such as photonic crystal [3] and air trenches [4] cannot.

This work provides insights into the design and fabrication issues relating to the ultra-compact grating-based beam splitter. It reveals the necessary approach to be taken in optimizing the beam splitter for more efficient CHOIR PICs in terms of reflectivity, loss, and interference extinction ratio. To the best of our knowledge, this is the first work to demonstrate that both low insertion loss and high interference extinction ratio are achievable using a grating-based beam splitter.

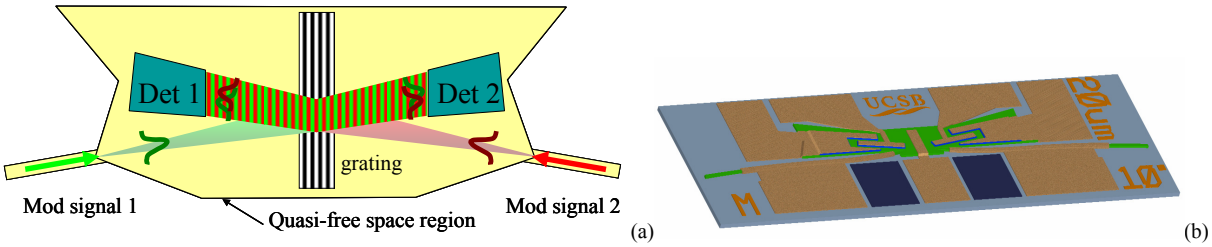

FIGURE 1. (a) Schematic diagram of grating-based beam splitter, integrated with two modulators and two photodetectors. Waveguide boundary is far away from the diverged beams in the quasi-free space region. Green and red colors represent input signals from the two modulators. (b) Fabricated grating-based beam splitter, including the modulators and photodetectors, shown to scale.

2. DESIGN AND FABRICATION

The design goal at hand is to realize an integrated beam splitter which has an equal splitting ratio, low insertion loss, short propagation length, as well as a high degree of interference between the output beams of two integrated multiple-quantum-well (MQW) phase modulators that are used in our CHOIR PICs, as shown in Fig. 1(a). Fig. 1(a) also shows the two integrated photodetectors used in the PIC, which are also used to obtain the measurements presented below. The simulations are based on 2-D, quasi-free space, two-wave interference method, as explained in [2]. One of the major issues with oblique incidence into a grating that is thick compared to the beam width is unequal mode distortion for the diffracted and undiffracted beams. This distortion comes from the continuous energy exchange in gratings [5]. In order to minimize degradation of interference due to this effect, two novel design techniques are used in this work: 1) the angle of incidence is made to be 10 degrees to the normal incidence, and 2)

the gratings are etched deep through the slab waveguide layer, which allows the grating region to be ultra short. Consequently, severe mode distortions can be avoided. In addition, the quasi-free space region shown in Fig. 1(a) is designed to provide for rapid beam divergence and, thus, for large beam-width-to-grating-length ratio.

The grating-based beam splitters are implemented on an InGaAsP/InP integration platform as illustrated in Figure 1 (b). The gratings are patterned on a SiO_2 hard mask using holographic exposure and then transferred by methane/hydrogen/argon (MHA)-based reactive ion etching (RIE) with oxygen addition [6]. Due to the non-uniformity of the photoresist at the edge of the grating burst, the actual grating lengths are 5 μm shorter than expected. The largest index contrast in the grating is achieved when the slab waveguide layer is completely etched through. As shown in [2], the etch of the deep grating grooves is followed by a regrowth of an InP cladding layer without apparent air voids, which suggests low void-stimulated scattering losses in our devices. An array of PICs containing grating-based beam splitters of various lengths and detectors of various widths has been fabricated and measured in this study, as explained below.

3. RESULTS AND DISCUSSION

Figure 2 shows the reflectivity spectra, plotted versus wavelength detuning from the Bragg wavelength, for the beam splitter having three different grating lengths (*Lg*) of 5 *μm*, 10 *μm*, and 15 *μm* and integrated with three different detectors having widths of 7 *μm* (*S*), 12 *μm* (*M*), and 23 *μm* (*L*). The middle grating length (*Lg*=10 *μm*) is designed to match the width of the optical beam incident on it, and the middle detector width (12 *μm*) is designed to match the width of its incident beam incident on it. The three detectors have the same length of 100 *μm*, which is long enough to absorb most of the light.

***Reflection**:* In the cases when *Lg* = 5 *μm* and *Lg* = 10 *μm*, the peak reflectivities for all three detector widths are typical of those for thin gratings and small incident angles. As the grating length gets larger than the interacting beam width, as is the case for *Lg* = 15 *μm*, the mode profiles of the reflected and transmitted waves experience unequal distortions [5], which also explains the difference in the data for the three detectors. The same data can be fitted to the well known *tanh*-relation [7] between reflectivity and κ**Lg*, with some reasonable assumptions, as shown in Fig. 3 (a). We assume that the κ value is 85% of the ideal case where a rectangular grating profile and a completely-etched-through slab waveguide are used. In our devices, because of the practical fabrication issues, we observe a certain degree of inevitable round up in the grating profile that results from the regrowth step, as shown in [2], and we also observe that the slab waveguide layers are not completely etched through. In addition, the reflectivity is assumed to saturate at 72%, as the overlap between the grating thickness and the mode profile in the transverse plane is not unity and some parts of the incident wave are transmitted through the deep grating region without experiencing any interference [8].

***Loss**:* The insertion loss data shown in Fig. 3 (b) provides information about: 1) propagation losses between the modulators and detectors, 2) scattering losses of the gratings, and 3) detector coupling losses, which are due to mismatches between the mode shapes and detector input areas. The propagation loss should be identical in all the cases studied since the waveguide geometry is kept the same. The coupling loss for the detector *L* can be assumed to be independent of the mode profile, since most of the incident light can be collected. Consequently, the insertion loss data obtained for the widest detector in Fig. 3(b) indicate that there is a small dependence of the scattering loss on the grating length. For the detector *M*, most of the incident light is still collected for all gratings lengths, except for some marginal loss due to the mode distortion in longer gratings. The material propagation loss can be estimated

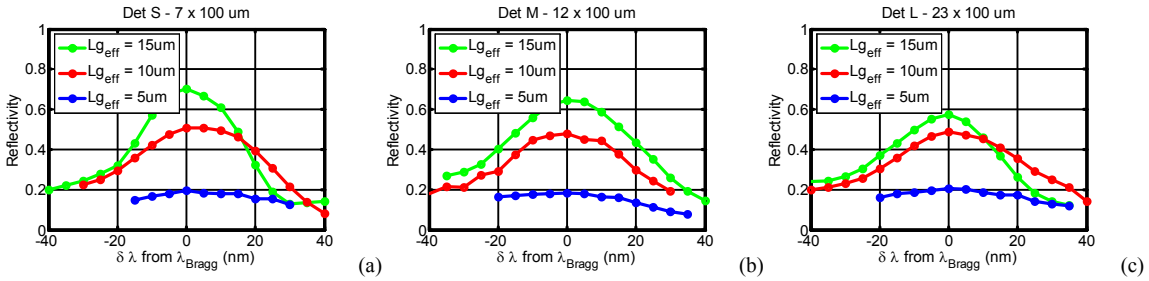

FIGURE 2. Reflectivity data with different grating lengths and detector widths. (a) Detector *S* width = 7 *μm* (b) Detector *M* width = 12 *μm* (c) Detector *L* width = 23 *μm*.

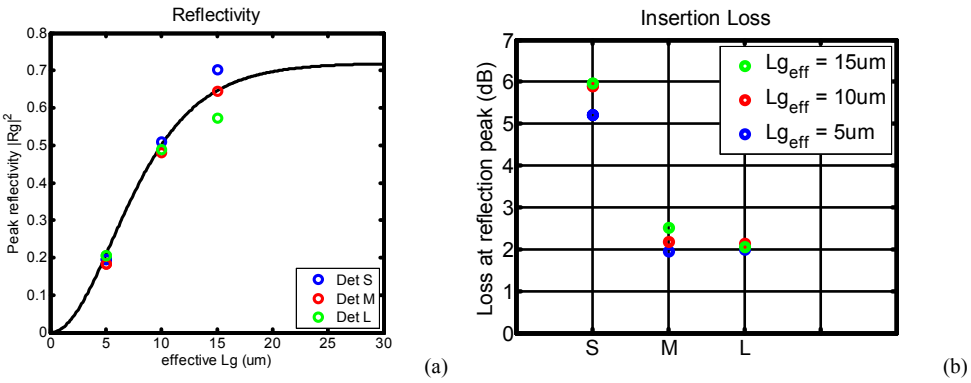

FIGURE 3. Bragg condition data. (a) Peak reflectivity. Circles are data from Figure 2 with different grating lengths and detector widths. Solid line represents the reflectivity *tanh* relation [7]. (b) Insertion loss for different detector widths: Detector *S* (7 μm), Detector *M* (12 μm), and Detector *L* (23 μm).

to be 0.5 dB.If we also take waveguide scattering losses into account, the grating scattering loss alone can be estimated to be less than 1.5 dB. For the detector *S*, excess coupling losses of about 3 to 4 dB for different grating lengths are measured, as expected, because only a portion of the incident light is captured due to the small detector width.

***Extinction Ratio**:* The interference behavior of the two beams coming from the two nominally identical MQW phase modulators is characterized by the extinction ratio between their constructive and destructive interferences. The extinction ratios are obtained by measuring the photocurrents of the detectors at their optimal operation points. The highest measured extinction ratios for the detector *L*, *M* and *S* are 6.5 dB, 13.5 dB and over 16 dB, respectively. Because the grating distorts the reflected and transmitted modes differently, the narrowest detector has the best extinction ratio as it mostly captures the parts of the modes that interfere most effectively. Therefore, with a proper choice of the detector width, both low insertion loss and high extinction ratio in our PICs can be achieved with deeply etched grating-based beam splitters. For example, for the 10-μm long grating and 12-μm wide photodetector, both 50% reflectivity (see Fig. 3(a)) and 2 dB insertion loss (see Fig. 3(b)) can be achieved for an extinction ratio as large as 13.5 dB.

4. CONCLUSION

In this paper, we have presented a comprehensive study of the ultra-compact grating-based beam splitter, where we were able to experimentally confirm our theoretical predictions. We have demonstrated beam splitters having 50% reflectivity and insertion loss as low as 2 dB. These ultra-short devices are only 10 μm long, and are invaluable for applications such as our CHOIR PICs, where they provide loop stability for high-frequencies, which cannot be easily achieved with competing technologies, in addition to larger than 13.5 dB extinction ratio. Moreover, the work provides design guidelines for future integrated grating-based beam splitters.

5. REFERENCES

[1] A. Ramaswamy, et al., "Coherent Receiver Based on a Broadband Optical Phase-Lock Loop," *OFC Conference* post deadline paper, 2007.

[2] C. H. Chen, et al., "Ultra-compact Grating-based 2x2 Beam Splitter for Miniature Photonic Integrated Circuits," The 20th Annual Meeting of IEEE *LEOS* 2007.

[3] S. Shi, et al., "Dispersion-based beam splitter in photonic crystals," *Optics Letters*, Vol. 29, No. 6, March 2004.

[4] Y. Lin, et al., "Compact and high efficiency polymer air-trench waveguide bends and splitters," *Proceedings of SPIE,* Vol. 6462, March 2007.

[5] M. R. Wang, "Analysis and observation of finite beam Bragg diffraction by a thick planar phase grating," *Applied Optics*, Vol. 35, No. 4, pp. 582-592, Feb. 1996.

[6] J. E. Schramm, et al., "Fabrication of high-aspect-ratio InP-based vertical-cavity laser mirrors using $CH_4/H_2/O_2/Ar$ reactive ion etching," *Journal of Vacuum Science & Technology B: Microelectronics and Nanometer Structures*, Vol. 15, No. 6, pp. 2031-2036, Nov. 1997.

[7] S. W. *Corzine*, et al., "A tanh substitution technique for the analysis of abrupt and graded interface multilayer dielectric stacks," *Journal of Quantum Electronics*, Vol. 27, No. 9, pp. 2086-2090, Sep. 1991.

[8] J. Ctyroky, et al., "Analysis of a deep waveguide Bragg grating," *Optical and Quantum Electronics*, Vol. 30, pp. 343-358, May 1998.